Edge Stability of BN sheets and Its Application for Designing Hybrid BNC Structures

Bing Huang[1], Hoonkyung Lee[2], Bing-Lin Gu[1], Feng Liu[3], and Wenhui Duan[1*]

[1]*Department of Physics, Tsinghua University, Beijing 100084, P. R. China*

[2]*Department of Physics, University of California,*

Berkeley, California 94720, USA and

[3]*Department of Materials Science and Engineering,*

University of Utah, Salt Lake City, Utah 84112, USA

(Dated: November 30, 2010)

Abstract

First-principles investigations on the edge energies and edge stresses of single-layer hexagonal boron-nitride (BN) are presented. The armchair edges of BN nanoribbons (BNNRs) are more stable in energy than zigzag ones. Armchair BNNRs are under compressive edge stress while zigzag BNNRs are under tensile edge stress. The intrinsic spin-polarization and edge saturation play important roles in modulating the edge stability of BNNRs. The edge energy difference between BN and graphene could be used to guide the design of the specific hybrid BNC structures: in an armchair BNC nanoribbon (BNCNR), BN domains are expected to grow outside of C domains, while the opposite occurs in a zigzag BNCNR. More importantly, armchair BNCNRs can reproduce unique electronic properties of armchair graphene nanoribbons (GNRs), which are expected to be robust against edge functionalization or disorder. Within certain C/BN ratio, zigzag BNC-NRs may exhibit intrinsic half-metallicity without any external constraints. These unexpected electronic properties of BNCNRs may offer unique opportunities to develop nanoscale electronics and spintronics beyond individual graphene and BN. Generally, these principles for designing BNC could be extended to other hybrid nanostructures.

* E-mail: dwh@phys.tsinghua.edu.cn

I. INTRODUCTION

Both single-layer boron-nitride (BN) sheet and graphene are two-dimensional (2D) crystals. Different from graphene, a zero-gap semimetal, BN sheet displays insulating characteristics due to the large ionicity of B and N atoms. Few-layers BN was first obtained by decomposition of borazine on metal surfaces with a matching lattice or in a mesh structure in the case of a lattice mismatch[1]. Much recent efforts have been made to synthesize single-layer BN. Free-standing BN single layers were fabricated in experiments via controlling energetic electron beam irradiation through a sputter process[2]. Similar to the graphene nanoribbons (GNRs), which are patterned from graphene via lithographical methods[3–5], it is possible to obtain BN nanoribbons (BNNRs) by cutting single-layer BN sheet.

The unusual electronic and magnetic properties of GNRs and BNNRs have been widely studied: both theoretical and experimental investigations reveal that all narrow GNRs are semiconducting regardless of their chirality (edge shapes)[3, 6–8]; meanwhile, zigzag GNRs (ZNGRs) are predicted to have magnetic ground states, while armchair GNRs (AGNRs) are nonmagnetic[7]. Similar to AGNRs, armchair BNNRs (ABNNRs) also display nonmagnetic semiconducting behavior independent of their width[9]; different from ZGNRs, however, zigzag BNNRs (ZBNNRs) could be either magnetic or nonmagnetic depending sensitively on their edge passivation[9–11].

Besides their electronic properties, further understanding of the edge stability of GNRs and BNNRs is necessary and important for practical device applications. The edge of a 2D structure is in analogy to the surface of a 3D structure and the edge stability can be potentially understood through two fundamental thermodynamic quantities: edge energy and edge stress, which defines the chemical and mechanical edge stability, respectively. The two quantities may interplay with each other affecting various edge-related phenomena in 2D structures. Some attention has already been paid to the edge instability of GNRs both in experiments[12] and theories[13–15]. It is found that AGNRs are more stable than ZGNRs in edge energy, and both are under intrinsic compressive edge stress, which results in edge twisting and warping instability[13–15]. Edge reconstruction or edge saturation could effectively lower the edge energies as well as relieve the edge compression and hence to stabilize the edge structures of GNRs[14, 15]. Comparing with GNRs, BNNRs have similar geometry but quite different electronic properties, and thus we expect some essential

differences in the edge stability between BNNRs and GNRs. In particular, the edge stability of BN structures have not been fully explored yet.

In this article, we systematically study the edge energies and edge stresses of BN sheet using first-principles calculations. Our results show that ABNNRs are more stable in energy than ZBNNRs. ABNNRs are under compressive stress, but ZBNNRs are under tensile stress. More interestingly, the intrinsic spin-polarization and edge adsorption of H could effectively stabilize the edges of BNNRs. Furthermore, using the edge energy difference between BN and graphene, we develop some basic principles for designing the structures of hybrid BNC[16]. Specifically, taking BNC nanoribbons (BNCNRs) as model systems, we find that in armchair BNCNRs (ABNCNRs), BN components are expected to form the armchair edges (with C components inside) to attain the lowest energy; while, C edges are preferred over BN edges in zigzag BNCNRs (ZBNCNRs). The hybrid BNCNRs show rich electronic and magnetic properties depending on their structures and the C/BN ratio. ABNCNRs can reproduce the basic electronic properties of AGNRs, and ZBNCNRs can exhibit half-metallicity within certain C/BN ratio. Thus, the hybrid BNC structures offer more opportunities than individual graphene and BN for building nano-scale electronics and spintronics.

II. COMPUTATIONAL METHODS AND MODELS

Our calculations were performed using density functional theory (DFT) in the generalized gradient approximation, with the Perdew-Burke-Ernzerhof (PBE) functional[17] for electron exchange and correlation potentials, as implemented in the VASP code [18]. The electron-ion interaction was described by the projector augmented wave (PAW) method[19], and the energy cutoff was set to 500 eV. The structures were fully optimized using the conjugate gradient algorithm until the residual atomic forces to be smaller than 10 meV/Å. The supercell with periodic boundary conditions was adopted to model the nanoribbons, with a vacuum layer larger than 15 Å to eliminate the interaction between the ribbon images in the neighboring cells.
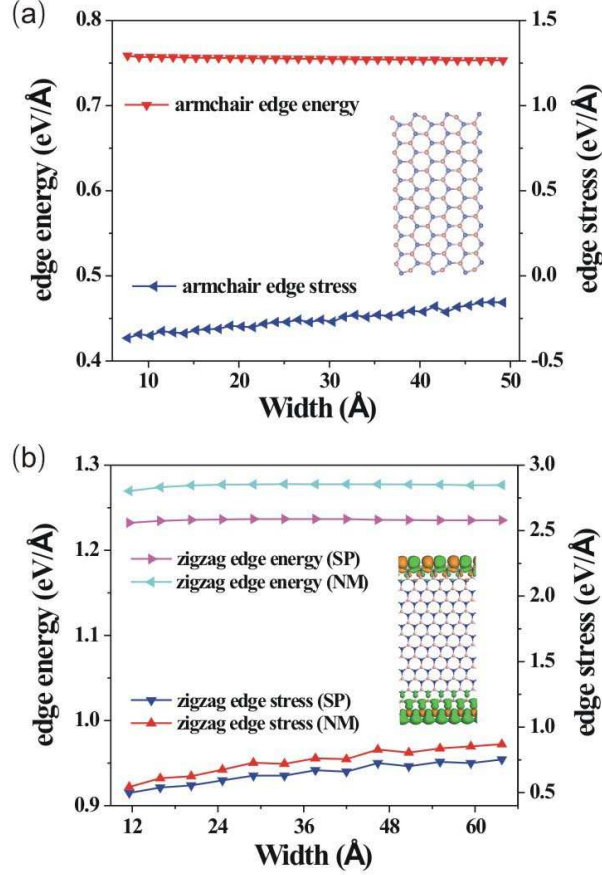
FIG. 1: (a) The edge energies and edge stresses of ABNNRs as a function of ribbon width. Inset: schematics of the optimized ABNNR. Blue and pink balls represent N and B atoms, respectively. (b) The spin-polarized (SP) and nonmagnetic (NM) edge energies and edge stresses of ZBNNRs as a function of ribbon width. Inset: schematics of the optimized ZBNNR associated with the spatial distribution of spin density of SP state. Green and orange colors represent the spin-up and spin-down states, respectively.

III. RESULTS AND DISCUSSION

Edge Stability of BN Sheets. Figure 1a shows the edge energies and edge stresses of bare ABNNRs with the width ranging from 7.5 to 50 Å. Herein, the edge energy of a bare BNNR is calculated as

$$E_{\text{edge}} = \frac{E_{\text{BNNR}} - \frac{N}{2}\varepsilon_{\text{BN}}}{2L} \tag{1}$$

where E_{BNNR} denotes the total energy of a BNNR with N boron and N nitrogen atoms in the supercell, ε_{BN} is the energy of a pair of BN atoms in a perfect BN sheet, and L is

the length of an edge. The edge stress is extracted from the calculated stress tensor by Nielsen-Martin algorithm[20], as described in previous work[15]. The edges of bare ABNNR are reconstructed (inset structure of Figure 1a): all B atoms at the edge relax inward and adjacent N atoms are outward away from the edge. The ground states of bare ABNNRs are nonmagnetic because the dangling-bonds are passivated after edge reconstruction. The average edge energy of ABNNRs, ~ 0.75 eV/Å, displays a weak width dependence, and is smaller than that of AGNRs (~ 1.0 eV/Å)[15, 21]. The edge stresses of ABNNRs are negative (i.e., compressive stress) and oscillate weakly (~ 0.02 eV/Å) with increasing ribbon width. The average edge stress of ABNNRs (~ -0.25 eV/Å) is much smaller than that of AGNRs (~ -1.45 eV/Å)[15], indicating that the armchair edges of BN are mechanically more stable than that of AGNRs. Moreover, the weak width-dependence of edge energies and edge stresses in ABNNRs are quite different that of AGNRs[15].

Figure 1b shows the calculated edge energies and edge stresses of ZBNNRs for different ribbon width ($11 \sim 64$ Å). The nonmagnetic edge energy is independent of ribbon width (~ 1.28 eV/Å), but the nonmagnetic edge stress increases by ~ 0.3 eV/Å as the ribbon width increases from ~ 11 to ~ 64 Å. The positive edge stress means that ZBNNRs are under intrinsic tensile stress, which is evidently different from that of ABNNRs. The ground states of bare ZBNNRs are spin-polarized with antiferromagnetic spin ordering at B-edge (i.e., the outmost atoms at the edge are B atoms) and ferromagnetic spin ordering at N-edge (i.e., the outmost atoms at the edge are N atoms), as shown in the inset of Figure 1b, in agreement with previous predictions[10, 11]. The magnetic moment is ~ 1 μB per edge B or N atom. The spin-polarized edge energies are ~ 0.04 eV/Å lower than the nonmagnetic ones. Furthermore, spin-polarization has a sizable effect of reducing the stress by ~ 0.1 eV/Å.

Previous studies demonstrated that both armchair and zigzag edges of graphene are under intrinsic compressive stress, resulting in edge twisting and warping instability[13–15]. Different from graphene, edge warping is expected to appear only at the armchair edges of BN (compressive edge stress) but not at the zigzag edges of BN (tensile edge stress). This indicates that the armchair and zigzag edges of BN should be distinguishable by their different edge morphologies (undulations) in experiments.

It is known that edge adsorption of H in GNRs can relieve the edge compression and lower the edge energies[14, 15, 21], because the compressive edge stress of GNRs originate from
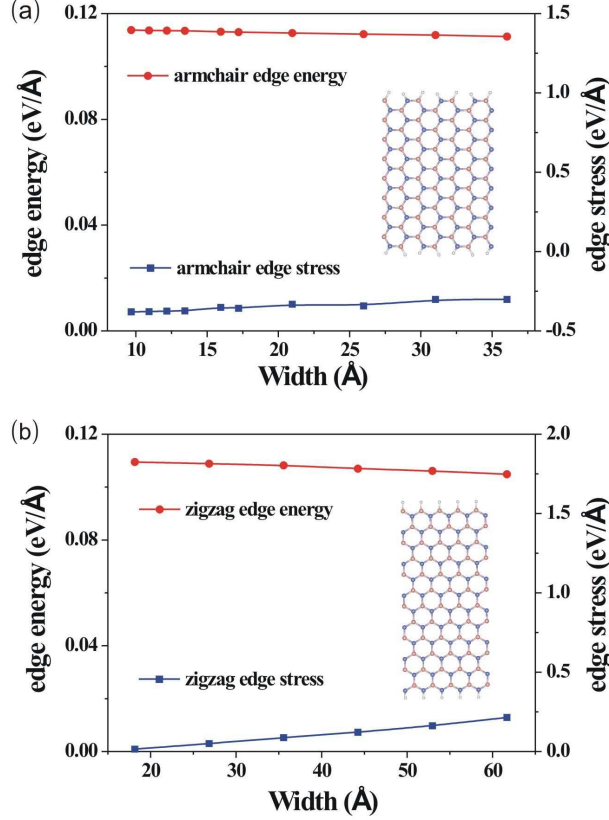
FIG. 2: The edge energies and edge stresses of (a) H-terminated ABNNRs and (b) H-terminated ZBNNRs as a function of ribbon width. Insets: schematics of the optimized ABNNR and ZBNNR.

the dangling bonds of bare edge atoms. Thus, we further investigate the effect of hydrogen passivation on the edge stability of BNNRs. The edge energy of a H-terminated BNNR is calculated as

$$E_{\text{edge}} = \frac{E_{\text{H-BNNR}} - \frac{N}{2}\varepsilon_{\text{BN}} - n_{\text{H}}\mu_{\text{H}}}{2L} \tag{2}$$

where $E_{\text{H-BNNR}}$, N, ε_{BN}, and L have the same definition as in Eq. (1). μ_{H} is the chemical potential of hydrogen and n_{H} is the number of H atoms in a supercell. Here, μ_{H} is calculated as half of the total energy of an isolated H_2 molecule. As shown in Figure 2a, the average edge energy of ABNNRs decreases largely from ~ 0.75 eV/Å to ~ 0.11 eV/Å after H adsorption, but the edge stress changes little. For ZBNNRs, the average edge energy is around 0.11 eV/Å, almost the same as ABNNRs; the edge stresses are reduced largely by ~ 0.50 eV/Å, as shown in Figure 2b. Notably, the edge passivation destroys the magnetic states of ZBNNRs, and the ground states is now nonmagnetic [10]. The above results strongly indicate that edge saturation could be used to stabilize the edges of BNNRs, similar to the

5

case of GNRs.

Geometries, Electronic and Magnetic Properties of Hybrid BNC Sheets. The edge energy difference between BN and graphene is useful to analyze the stability of hybrid BNC structures. Under equilibrium growth conditions, BN and C are thermodynamically immiscible, preferring to separate into domains in planar BNC structures[16, 22]. For armchair edges, since the edge energies of ABNNRs (~ 0.75 eV/Å) are much lower than those of AGNRs (~ 1.0 eV/Å), BN prefers to form the edges while C stays inside to lower the overall energy. However, the situation is totally different for zigzag edges of BNC structures, as C prefers to form the edges with BN staying inside, because of the lower edge energies of ZGNRs. It should be noted that the B, N, and C atoms in BNC sheet containing substitutional C atoms were identified in a very recent experiment[23]. Therefore, we highly expect the future experiments to identify the edge atomic species of hexagonal BNC structures to support our prediction. In the following, we will take BNCNRs as examples to verify these simple predictions in theory and systematically study the electronic properties of BNCNRs.

As shown in Figure 3a and Figure 5a, a simple BNCNR consists of BNNR domains and GNR domains. Following the conventional notations of m-BNNR and n-GNR, an armchair (a zigzag) BNCNR is defined as (m, n) ABNCNR (ZBNCNR), with m and n dimer lines (zigzag chains) across the BN and C ribbon width, respectively. For example, the structures in Figure 3a and Figure 5a are referred as armchair $(16, 8)$ ABNCNR an $(6, 6)$ ZBNCNR, respectively. In this article, we focus on the specific BNCNR configurations that either BN or C grows at both ribbon edges. In addition, we concentrate our attention on these situations that BN (or C) stay at both BNCNR edges symmetrically, since our test calculations indicate that symmetrical distributions of BN (or C) at both edges are more favorable in energy than other asymmetrical ones.

In the following, $(16, 16)$ ABNCNRs are taken as examples for BNCNRs with armchair edges. The component of BNNRs (or GNRs) could be either outside or inside, namely, the edge atoms could be either C (ABNCNR-CC) or BN (ABNCNR-BN). The calculated total energies in the two cases indeed confirm our analysis based on the large edge energy differences between graphene and BN: ABNCNR-BN is 1.86 eV per unit cell (~ 0.22 eV/Å) lower in energy than ABNCNR-CC, indicating that the differences of BN-C domain interfacial energy as well as inter-domain interaction energy for the two cases are small (~ 0.03 eV/Å)[16].
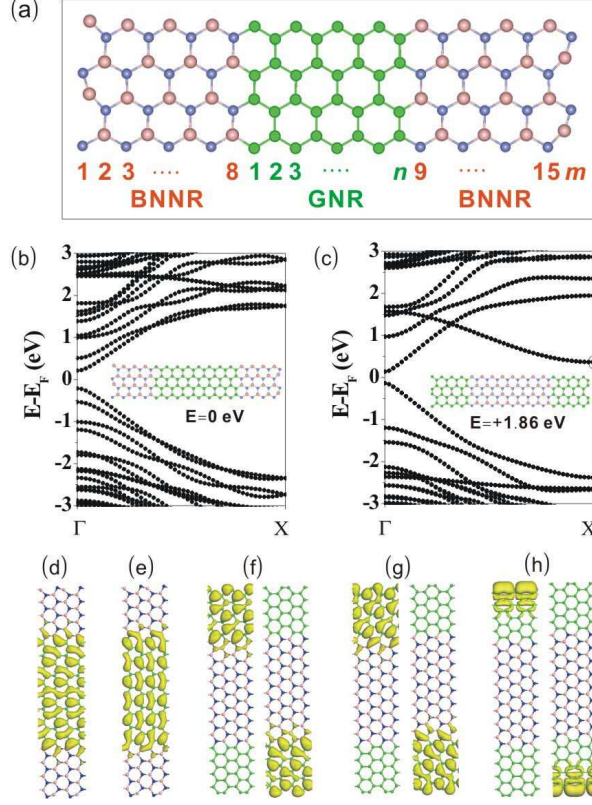
FIG. 3: (a) The schematic structure of (m, n) ABNCNR with m and n dimer lines for the BNNR and GNR, respectively; Blue, pink, and green balls represent N, B, and C atoms, respectively. (b) and (c) are the band structures of (16, 16) ABNCNR-BN and (16, 16) ABNCNR-CC, respectively. The Fermi level is set to zero. The corresponding optimized atomic structures and relative total energies are also shown as an inset in (b) and (c). (d) and (e) are partial charge densities of the top valence band and the bottom conduction band at the Γ point of (16, 16) ABNCNR-BN, respectively. (f) and (g) are partial charge densities of the top valence band and the bottom conduction band at the Γ point of (16, 16) ABNCNR-CC, respectively. (h) Partial charge density of the bottom conduction band at the X point of (16, 16) ABNCNR-CC.

The calculated band structures, as shown in Figure 3b and c, demonstrate that both structures are nonmagnetic semiconductors with a direct bandgap of ~ 0.42 eV (Figure 3b) and ~ 0.27 eV (Figure 3c). BNNRs are insulating with a bandgap > 4 eV (based on our calculation), which is much larger than that of GNRs[7, 24], so BN domain in a BNCNR may act as "energy barrier" to confine the states of GNR component around the Fermi level. Similar physical mechanism has been found in partially hydrogenated graphene[25],

7

but precise control of the distribution of hydrogen atoms on the graphene surface is rather challenging. The partial charge density analysis confirms that the bands around the Fermi level are mostly localized in the GNR domains, as shown in Figure 3d-3g [the states of (16, 16) ABNCNR-CC around the Fermi level are doubly-degenerate]. Moreover, a state near the bottom of conduction band in Figure 3c has a small dispersion with a flattened tail near the X-point and the partial charge density of the two doubly-degenerate states at X-point are localized around the two armchair edges of GNR domains (Figure 3h), belonging to the "edge states", which may be caused by the chemical potential difference between the two boundaries of GNR domain. The edge states were only found at the zigzag edges of graphene previously[26], and have exhibited plenty of important applications[6, 27, 28]. Surprisingly, our results here demonstrate that it is also possible to introduce edge states at the armchair edges of graphene via hybrid BNC structures. Furthermore, doping electrons to the system (or other chemical functionalization) may pull down the armchair edge states to the Fermi level for further applications. Although the structures of ABNCNRs-CC are less stable in energy than ABNCNRs-BN, it is still possible to realize them in experiments under non-equilibrium growth conditions via controlling the deposition rate, temperature and the effect of substrate[16].

Since the states of ABNCNRs around the Fermi level mainly originate from GNR domains, we expect that the well known features of AGNRs could be reproduced in ABNCNRs. For instance, it is known that the energy gaps of AGNRs decrease as ribbon width increases and exhibit three distinct family behaviors[7, 24], and we expect the similar quantum confinement effect could also exist in ABNCNRs. The calculated band gaps of $(16, n)$ ABNCNRs-BN with different n (width of the GNR part) are shown in Figure 4a. The band gaps of hybrid ABNCNRs could be divided into three groups and decrease with the increase of the width, similar to the case of AGNRs. Different from the gap size hierarchy of AGNRs ($\triangle_{3p+1} > \triangle_{3p} > \triangle_{3p+2}$)[7, 24], the hierarchy of ABNCNRs is $\triangle_{3p} > \triangle_{3p+1} > \triangle_{3p+2}$. The discrepancy may come from the essential differences between the edges of GNRs and the boundaries of BNCNRs, as found in previous work[29, 30]. Besides, the bandgap values of ABNCNRs are much smaller than those of the corresponding AGNRs. The band structures of $(16, n)$ ABNCNRs-BN ($n = 6, 7$, and 8) are shown in Figure 4b as examples.

Theoretical studies have predicted interesting electronics of GNRs with perfect edges[6]. Unfortunately, most of the intrinsic properties predicted have not been observed in experi-
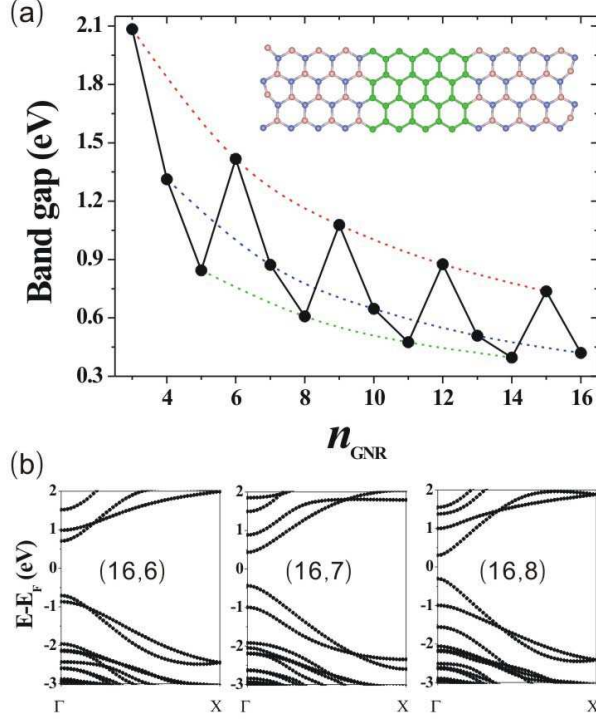
FIG. 4: (a) The band gaps of $(16, n)$ ABNCNRs-BN as a function of n (the width of the GNR part). (b) Band structures of $(16, n)$ ABNCNRs-BN ($n = 6$, 7, and 8). The Fermi level is set to zero.

ments until now, because it is very difficult to get smooth edges under current experimental technology[3, 4]. The rough edge structures will dramatically influence the electronic properties of GNRs[6, 31]. Besides, edge chemical functionalization as well as doping is also inevitable in experiments due to the high chemical reactivity of the graphene edges[3, 4, 32]. Quite encouragingly, our study strongly implies that ABNCNRs can exhibit novel electronic properties of prefect GNRs: since the BN prefers to grow outside of GNRs and the electronic properties of BN are robust against different chemical functionalization[33, 34], the electronic properties of ABNCNRs, mimicking those of AGNRs around the Fermi level, are expected to be also robust.

We now turn to ZBNCNRs. According to our prediction, C prefers to form the zigzag edges outside of BN. We take (8, 8) ZBNCNRs as examples and different BNC configurations have been considered, as shown in Figure 5. The case of C growing outside of BN is named as (8, 8) ZBNCNR-CC for short, as shown in Figure 5b. There are three different configurations for the cases of BN growing outside of C: (1) one edge is B-edge, and the
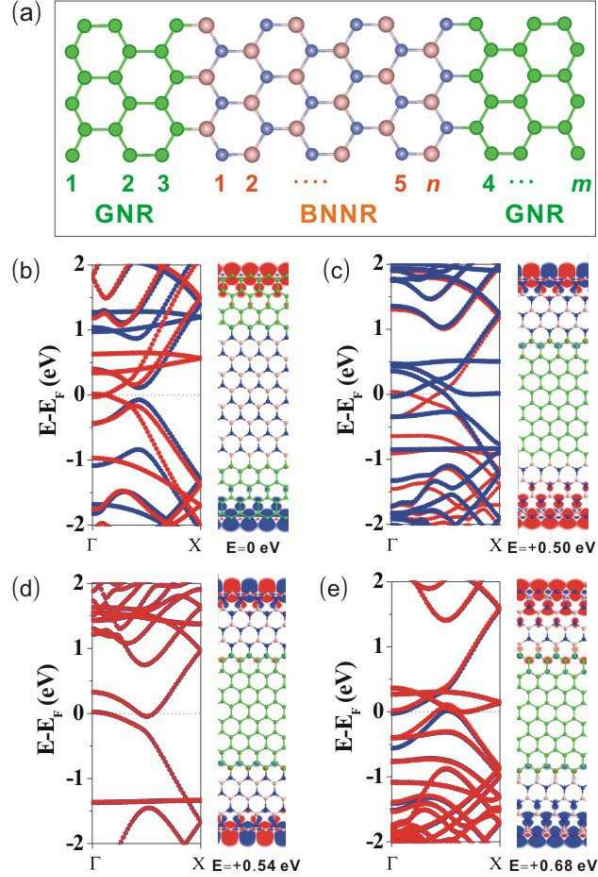
9

FIG. 5: (a) The schematic structure of (m, n) ZBNCNR with m and n zigzag chains for the BNNR and GNR, respectively. (b-e) The spin-polarized band structures of (b) (8, 8) ZBNCNR-CC, (c) (8, 8) ZBNCNR-BN, (d) (8, 8) ZBNCNR-BB, and (e) (8, 8) ZBNCNR-NN. The corresponding optimized atomic structures associated with the spatial distribution of (ground state) spin densities and the relative (ground state) total energies are also presented in (b)-(e). Blue and red colors represent the spin-up and spin-down states, respectively. The Fermi level is set to zero.

other edge is N-edge (ZBNCNR-BN, Figure 5c), (2) both edges are B-edges (ZBNCNR-BB, Figure 5d), (3) both edges are N-edges (ZBNCNR-NN, Figure 5e). Because specific magnetic orderings were found along the zigzag edges of GNRs and bare BNNRs[7, 10, 11], it is expected that spin-polarization will also play an important role in ZBNCNRs. In order to search for the most stable spin configurations, the total energies of ZBNCNRs with different initial spin orderings are calculated in double unit cell. The spin configurations that are most energetically favorable are displayed in Figure 5b-5e: for ZBNCNR-CC, spins have ferromagnetic ordering at each C-edge and antiferromagnetic coupling between two C-edges

10

(Figure 5b); for ZBNCNR-BN, spins have antiferromagnetic ordering at the B-edge and ferromagnetic ordering at the N-edge (Figure 5c); for ZBNCNR-BB, spins have antiferromagnetic ordering at both B-edges (Figure 5d); for ZBNCNR-NN, spins have ferromagnetic ordering at each N-edge and antiferromagnetic coupling between two N-edges (Figure 5e). The total energy of ZBNCNR-CC is more favorable than ZBNCNR-BN, ZBNCNR-BB, and ZBNCNR-NN by 0.50, 0.54, and 0.68 eV per double unit cell (i.e., $\sim$ 0.050, 0.054 and 0.068 eV/Å), respectively, consistent with our prediction that C prefers to form the zigzag edges in BNCNRs.

It is interesting to see that the ground state of (8, 8) ZBNCNR-CC exhibits intrinsic half-metallic behavior (Figure 5b), with an apparent gap ($\sim$ 0.2 eV) for the spin-up state and two bands crossing the Fermi level for the spin-down state. This mainly results from the large chemical potential difference between the C-B and C-N boundaries as well as the hybridization of the orbitals of C, B and N atoms at BN-C boundaries[30, 35]. Although there are already some reports on half-metallicity and ferromagnetism in various BN[10, 36] and hybrid BNC structures[30, 35], the feasibility of realizing these structures in practice (i.e., the stability of these structures) were unknown. Our work presents some new insights on understanding these hybrid BNC structures. Different from (8, 8) ZBNCNR-CC, (8, 8) ZBNCNR-BN (Figure 5c) is a ferromagnetic metal with $\sim$ 2 μB net magnetic moment per double unit cell, while (8, 8) ZBNCNR-BB (Figure 5d) and (8, 8) ZBNCNR-NN (Figure 5e) are antiferromagnetic metal with zero net magnetic moment per double unit cell. These results indicate that the electronic and magnetic properties of ZBNCNRs are strongly dependent on the detailed hybridized structures, which may be achieved in experiments under specific growth conditions.

Moreover, the existence of half-metallicity as well as the value of half-metallic gap in ZBNCNR-CC depends strongly on the C/BN ratio (i.e., n/m), as shown in Figure 6. Clearly, the half-metallic gap decreases from 0.27 eV (Figure 6a) to 0.19 eV (Figure 6b) to 0.12 eV (Figure 6c) by increasing the C/BN ratio from 33.3% to 60% to 100%, respectively. These half-metallic gaps are large enough for room-temperature operation. ZBNCNR-CC will convert from half-metal to ferromagnetic metal as the C/BN ratio is further increased (larger than 100%), as presented in Figure 6d and 6e. Thus, the electronic and magnetic properties of ZBNCNRs could be precisely modulated by changing the C/BN ratio.
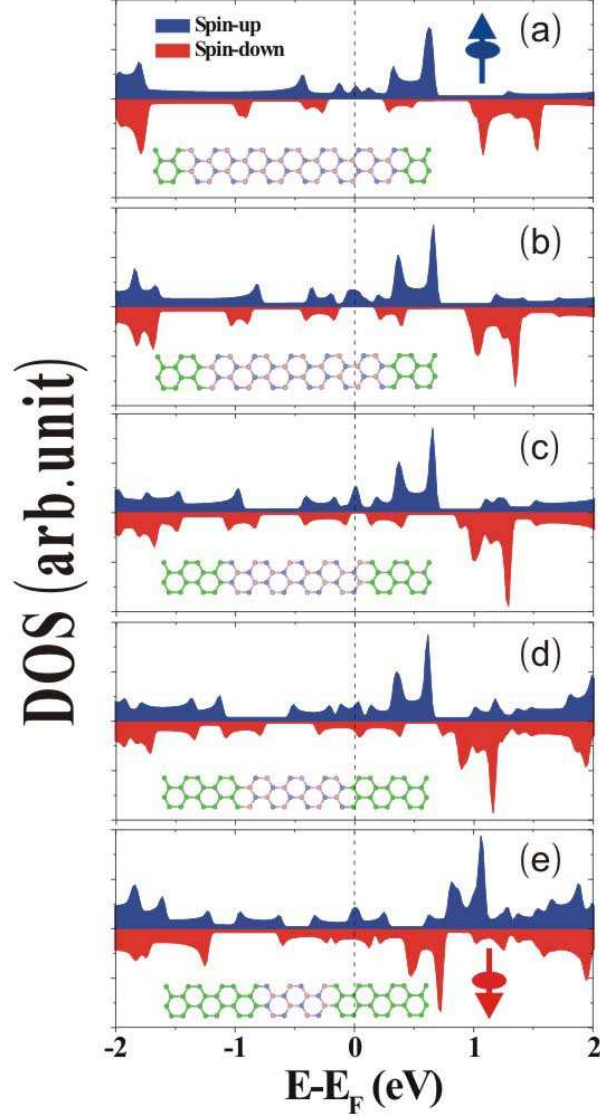
FIG. 6: The density of states of (a) (12, 4) ZBNCNR-CC, (b) (10, 6) ZBNCNR-CC, (c) (8, 8) ZBNCNR-CC, (d) (6, 10) ZBNCNR-CC, and (e) (4, 12) ZBNCNR-CC. The insets show the corresponding atomic structures. Blue and red colors represent spin-up and spin-down states, respectively. The Fermi level is set to zero.

IV. SUMMARY

In conclusion, using spin-polarized DFT calculations, we have systemically studied the edge stability (edge energy and edge stress) of single-layer BN. Our results demonstrate that the edges of ABNNRs are more stable than those of ZBNNRs. ABNNRs are under compressive edge stress but ZBNNRs are under tensile stress. The intrinsic spin-polarization

12

and edge adsorption of H could stabilize the edges of BNNRs. Furthermore, the different edge stability between BN and graphene may be used to provide some guiding principles for designing the specific structures of hybrid BNC. For examples, BN is expected to grow outside of C in ABNCNRs, while the reverse is true in ZBNCNRs. The hybrid BNCNRs show rich electronic and magnetic properties depending strongly on their detailed structures and the atomic C and BN ratio. Our findings can be useful for developing nanoscale electronics and spintronics.

Acknowledgments

[1] M. Corso, W. Auwarter, M. Muntwiler, A. Tamai, T. Greber, and J. Osterwalder, Science **303**, 217 (2004); A. Nagashima, N. Tejima, Y. Gamou, T. Kawai, and C. Oshima, Phys. Rev. Lett. **75**, 3918 (2009).

[2] C. Jin, F. Lin, K. Suenaga, and S. Iijima, Phys. Rev. Lett. **102**, 195505 (2009); J. C. Meyer, A. Chuvilin, G. Algara-Siller, J. Biskupek, and U. Kaiser, Nano Lett. **9**, 2683 (2009).

[3] M. Y. Han, B. Ozyilmaz, Y. Zhang, and P. Kim, Phys. Rev. Lett. **98**, 206805 (2007).

[4] Z. Chen, Y. M. Lin, M. J. Rooks, and P. Avouris, Physica E **40**, 228 (2007).

[5] L. Tapaszto, G. Dobrik, P. Lambin, and L. P. Biro, Nat. Nanotechnol. **3**, 397 (2008).

[6] A. H. Castro Neto, F. Guinea, N. M. R. Peres, K. S. Novoselov, and A. K. Geim, Rev. Mod. Phys. **81**, 109 (2009).

[7] Y.-W. Son, M. L. Cohen, and S. G. Louie, Phys. Rev. Lett. **97**, 216803 (2006).

[8] X. Wang, Y. Ouyang, X. Li, H. Wang, J. Guo, and H. Dai, Phys. Rev. Lett. **100**, 206803 (2008).

[9] C. H. Park and S. G. Louie, Nano Lett. **8**, 2200 (2008).

[10] F. W. Zheng, G. Zhou, Z. Liu, J. Wu, W. H. Duan, B. -L. Gu, and S. B. Zhang, Phys. Rev. B **78**, 205415 (2008).

[11] V. Barone and J. E. Peralta, Nano Lett. **8**, 2210 (2008).

[12] J. C. Meyer, A. K. Geim, M. I. Katsnelson, K. S. Novoselov, T. J. Booth, and S. Roth, Nature (London) **446**, 60 (2007); M. H. Gass, U. Bangert, A. L. Bleloch, P. Wang, R. R. Nair, and A. K. Geim, Nature Nanotech. **3**, 676 (2008); Z. Liu, K. Suenaga, P. J. F. Harris, and S. Iijima, Phys. Rev. Lett. **102**, 015501 (2009); J. Y. Huang, F. Ding, B. I. Yakobsonc, P. Lud, L. Qie, and J. Lie, Proc. Natl. Acad. Sci. **106**, 10103 (2009).

[13] V. B. Shenoy, C. D. Reddy, A. Ramasubramaniam, and Y. W. Zhang, Phys. Rev. Lett. **101**, 245501 (2008).

[14] K. V. Bets and B. I. Yakobson, Nano Res. **2**, 161 (2009).

[15] B. Huang, M. Liu, N. Su, J. Wu, W. H. Duan,and F. Liu, Phys. Rev. Lett. **102**, 166404 (2009).

[16] L. Ci, L. Song, L. Jin, D. Jariwala, D. Wu, Y. Li, A. Srivastava, Z. F. Wang, K. Storr, L. Balicas, F. Liu, and M. A. Ajayan, Nat. Mater. **9**, 430 (2010).

[17] J. P. Perdew, K. Burke, and M. Ernzerhof, Phys. Rev. Lett. **77**, 3865 (1996).

[18] G. Kresse and J. Furthmüller, Comput. Mater. Sci. **6**, 15 (1996).

[19] G. Kresse and D. Joubert, Phys. Rev. B **59**, 1758 (1999).

[20] O. H. Nielsen and R. M. Martin, Phys. Rev. B **32**, 3780 (1985).

[21] P. Koskinen, S. Malola, and H. Hakkinen, Phys. Rev. Lett. **101**, 115502 (2008).

[22] K. Yuge, Phys. Rev. B **79**, 144109 (2009).

[23] O. L. Krivanek, M. F. Chisholm, V. Nicolosi, T. J. Pennycook, G. J. Corbin, N. Dellby, M. F. Murfitt, C. S. Own, Z. S. Szilagyi, M. P. Oxley, S. T. Pantelides, and S. J. Pennycook, Nature (London) **464**, 571 (2010).

[24] Q. M. Yan, B. Huang, J. Yu, F. W. Zheng, J. Zang, J. Wu, B. L. Gu, F. Liu, and W. H. Duan, Nano Lett. **7**, 1469 (2007).

[25] A. K. Singh and B. I. Yakobson, Nano Lett. **9**, 1540 (2009); H. Xiang, E. Kan, S. -H. Wei, M. -H. Whangbo, and J. Yang, Nano Lett. **9**, 4025 (2009).

[26] K. Nakada, M. Fujita, G. Dresselhaus, and M. S. Dresselhaus, Phys. Rev. B **54**, 17954 (1996).

[27] Y. -W. Son, M. L. Cohen, S. G. Louie, Nature (London) **444**, 347 (2006); E. J. Kan, Z. Li, J. Yang, and J. G. Hou, J. Am. Chem. Soc., **130**, 4224 (2009).

[28] W. Y. Kim, and K. S Kim, Nat. Nanotech. **3**, 408 (2008); F. Munoz-Rojas, J. Fernandez-Rossier, and J. J. Palacios, Phys. Rev. Lett. **102**, 136810 (2009).

[29] A. Du, Y. Chen, Z. Zhu, G. Lu, and S. C. Smith, J. Am. Chem. Soc. **131**, 1682 (2009).

[30] B. Huang, C. Si, H. Lee, L. Zhao, J. Wu, B. -L. Gu, and W. H. Duan, Appl. Phys. Lett. **97**, 043115 (2010).

[31] B. Huang, Q. Yan, G. Zhou, J. Wu, B. -L. Gu, W. H. Duan, and F. Liu, Appl. Phys. Lett. **91**, 253122 (2007); B. Huang, F. Liu, J. Wu, B. -L. Gu, and W. H. Duan, Phys. Rev. B **77**, 153411 (2008); B. Huang, Z. Li, Z. Liu, G. Zhou, S. Hao, J. Wu, B. -L. Gu, and W. H. Duan, J. Phys. Chem. C **112**, 13442 (2008).

[32] X. Li, X. Wang, L. Zhang, S. Lee, and H. Dai, Science **319**, 1229 (2008).

[33] Y. Chen, J. Zou, S. J. Campbell, and G. L. Caer, Appl. Phys. Lett. **84**, 2430 (2004).

[34] X. Wu, W. An, and X. C. Zeng, J. Am. Chem. Soc. **128**, 12001 (2006).

[35] E. J. Kan, X. Wu, Z. Li, X. C. Zeng, J. Yang, J. G. Hou, J. Chem. Phys. **129**, 084712 (2008); J. Li, G. Zhou, Y. Chen, B. -L. Gu, and W. H. Duan, J. Am. Chem. Soc. **131**, 1796 (2009); S. Dutta, A. K. Manna, and S. K.Pati, Phys. Rev. Lett. **102**, 096601 (2009); J. M. Pruneda, Phys. Rev. B **81**, 161409 (2009); Y. Ding, Y. Wang, and J. Ni, Appl. Phys. Lett. **95**, 123105 (2009).

[36] A. Du, Y. Chen, Z. Zhu, R. Amal, G. Lu, and S. C. Smith, J. Am. Chem. Soc. **131**, 17354 (2009); Z. Zhang and W. Guo, J. Am. Chem. Soc. **131**, 6874 (2009); W. Chen, Y. Li, G. Yu, C. Z. Li, S. B. Zhang, Z. Zhou, and Z. Chen, J. Am. Chem. Soc. **132**, 1699 (2010).